Characterization of the roles of Blt1p in fission yeast cytokinesis

John W. Goss[a,b], Sunhee Kim[a], Hannah Bledsoe[b], and Thomas D. Pollard[a,c,d]
[a]Department of Molecular Cellular and Developmental Biology, [c]Department of Molecular Biophysics and Biochemistry, and [d]Department of Cell Biology, Yale University, New Haven, CT 06520-8103; [b]Department of Biological Sciences, Wellesley College, Wellesley, MA 02481-8203

ABSTRACT **Spatial and temporal regulation of cytokinesis is essential for cell division, yet the mechanisms that control the formation and constriction of the contractile ring are incompletely understood. In the fission yeast *Schizosaccharomyces pombe* proteins that contribute to the cytokinetic contractile ring accumulate during interphase in nodes—precursor structures around the equatorial cortex. During mitosis, additional proteins join these nodes, which condense to form the contractile ring. The cytokinesis protein Blt1p is unique in being present continuously in nodes from early interphase through to the contractile ring until cell separation. Blt1p was shown to stabilize interphase nodes, but its functions later in mitosis were unclear. We use analytical ultracentrifugation to show that purified Blt1p is a tetramer. We find that Blt1p interacts physically with Sid2p and Mob1p, a protein kinase complex of the septation initiation network, and confirm known interactions with F-BAR protein Cdc15p. Contractile rings assemble normally in *blt1Δ* cells, but the initiation of ring constriction and completion of cell division are delayed. We find three defects that likely contribute to this delay. Without Blt1p, contractile rings recruited and retained less Sid2p/Mob1p and Clp1p phosphatase, and β-glucan synthase Bgs1p accumulated slowly at the cleavage site.**

Monitoring Editor
Fred Chang
Columbia University

Received: Jun 4, 2013
Revised: Apr 14, 2014
Accepted: Apr 22, 2014

INTRODUCTION

The fission yeast *Schizosaccharomyces pombe* uses a highly conserved mechanism to assemble and constrict a cytokinetic contractile ring composed of actin filaments and myosin-II to divide by medial fission (Pollard and Wu, 2010). Preparation for cytokinesis begins during interphase, when key signaling proteins accumulate around the cell equator in cortical structures called interphase nodes. These node proteins include kinases Cdr1p, Cdr2p, and Wee1p, putative RhoGEF Gef2p, kinesin-like protein Klp8p, anillin-related protein Mid1p, and the presumed scaffolding protein Blt1p (Paoletti and Chang, 2000; Morrell *et al.*, 2004; Martin and Berthelot-Grosjean, 2009; Moseley *et al.*, 2009; Guzman-Vendrell *et al.*, 2013). At the onset of mitosis, interphase nodes mature into cytokinesis nodes upon recruitment of IQGAP protein Rng2p, myosin-II heavy chain Myo2p and light chains Rlc1p and Cdc4p, F-BAR protein Cdc15p, and formin Cdc12p (Wu *et al.*, 2003, 2006; Almonacid *et al.*, 2011; Laporte *et al.*, 2011; Padmanabhan *et al.*, 2011). Interactions between myosin-II and actin filaments polymerized by Cdc12p condense nodes into the contractile ring (Vavylonis *et al.*, 2008).

After contractile ring assembly, a signal transduction pathway called the septation initiation network (SIN) compacts the ring, initiates contractile ring constriction, and promotes the onset of septation during cytokinesis (Hachet and Simanis, 2008; Krapp and Simanis, 2008). The SIN uses a protein phosphorylation cascade that activates the NDR-family kinase Sid2p and its regulatory subunit Mob1p at the cleavage site (Sparks *et al.*, 1999; Hou *et al.*, 2000; Salimova *et al.*, 2000). Among the Sid2p kinase substrates is the Cdc14-family phosphatase Clp1p, which concentrates in the nucleus during interphase but moves to kinetochores, the mitotic spindle, and the cleavage site during mitosis (Clifford *et al.*, 2008). Sid2p phosphorylation of Clp1p contributes to its retention in the cytoplasm (Chen *et al.*, 2008). At the contractile ring, Clp1p dephosphorylates Cdc15p, causing conformation changes that contribute to compaction of the contractile ring and progression of cytokinesis (Clifford *et al.*, 2008; Roberts-Galbraith *et al.*, 2010). In

This article was published online ahead of print in MBoC in Press (http://www.molbiolcell.org/cgi/doi/10.1091/mbc.E13-06-0300) on April 30, 2014.

Address correspondence to: Thomas D. Pollard (thomas.pollard@yale.edu).

Abbreviations used: CFP, cyan fluorescent protein; GAP, GTPase-activating protein; GEF, guanine nucleotide exchange factor; GFP, green fluorescent protein; RFP, red fluorescent protein; SIN, septation initiation network; SPB, spindle pole body; YFP, yellow fluorescent protein.

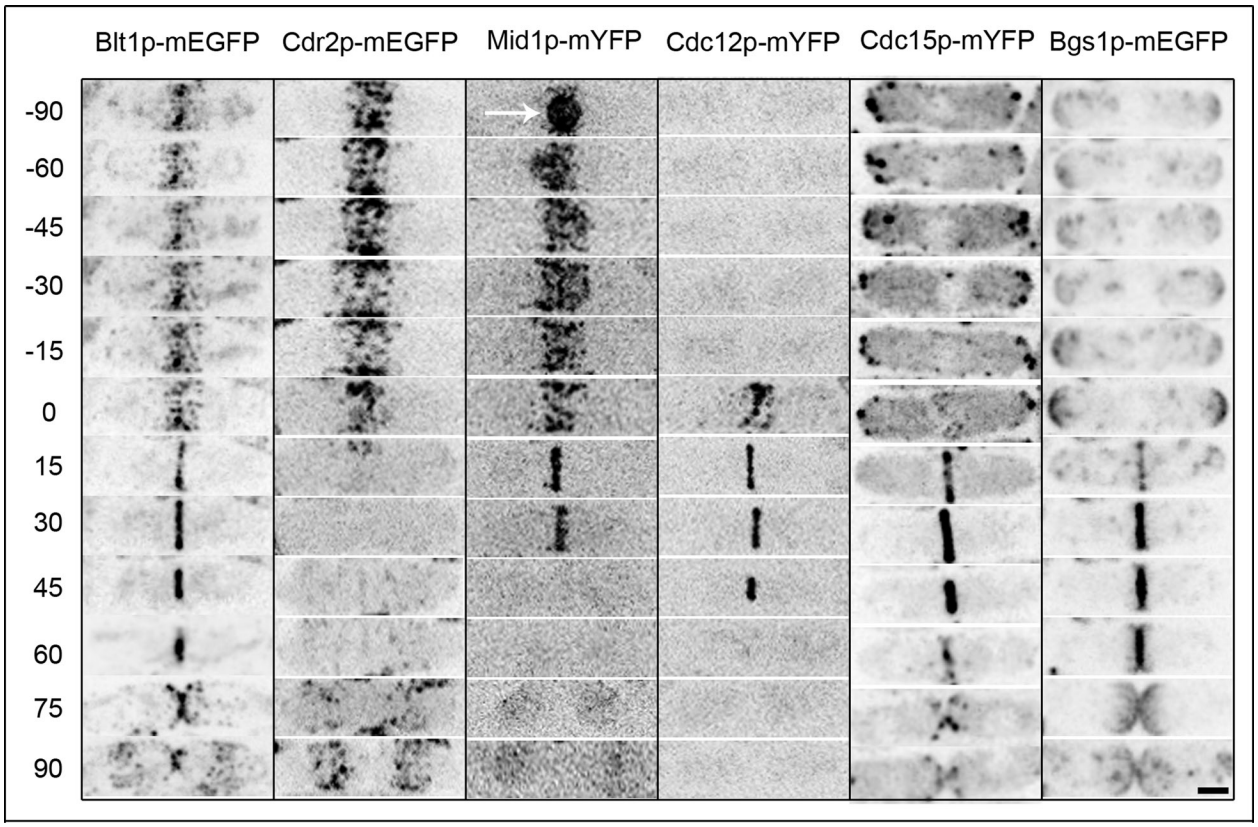

FIGURE 1: Localization of Blt1p across the cell cycle relative to other node and contractile ring proteins. Time series of reversed contrast fluorescence micrographs taken at 2-min intervals and displayed at 15- or 30-min intervals of one representative series from ≥20 wild-type cells examined expressing Blt1p-mEGFP, Cdr2p-mEGFP, Mid1p-mYFP, Cdc12p-mYFP, Cdc15p-mYFP, or Bgs1p-mEGFP. Time is in minutes, with spindle pole body separation defined as time zero. Arrow indicates Mid1p-mYFP in the nucleus. Scale bar, 2.5 μm.

addition, SIN signaling regulates the accumulation of (1,3)β-D-glucan synthase Bgs1p/Cps1p in the plasma membrane adjacent to the contractile ring, where the enzyme synthesizes the primary septum (Liu *et al.*, 1999; Le Goff *et al.*, 1999; Cortes *et al.*, 2002; Jin *et al.*, 2006). Synthesis of the primary septum in the cleavage furrow contributes to the inward force driving constriction of the contractile ring (Liu *et al.*, 1999; Proctor *et al.*, 2012). Although much is known about the assembly of interphase and cytokinesis nodes and SIN signaling, the mechanisms coordinating cytokinesis are poorly understood.

Blt1p is intriguing because it is one of the few proteins present in structures related to cytokinesis throughout the entire cell cycle. Although not essential for viability, Blt1p contributes to anchoring interphase node proteins Gef2p and Mid1p in the cell cortex (Moseley *et al.*, 2009; Ye *et al.*, 2012; Guzman-Vendrell *et al.*, 2013; Jourdain *et al.*, 2013), and all three proteins are incorporated in the contractile ring, whereas other interphase node proteins disperse into the cytoplasm (Moseley *et al.*, 2009). This persistence in the contractile ring suggested that Blt1p might have additional, unidentified functions later in mitosis.

We report that cells lacking Blt1p assemble contractile rings normally but initiate and complete cleavage later than do wild-type cells. We identify roles for Blt1p in recruiting Sid2p/Mob1p protein kinase complex, phosphatase Clp1p, and glucan synthase Bgs1p to the cleavage site. Without Blt1p, all of these proteins accumulate slowly around the middle of the cell, likely contributing to the delay in cytokinesis.

RESULTS

Localization of Blt1p across the cell cycle

We localized Blt1p and other cytokinesis proteins in live cells throughout the cell cycle by tagging each protein with a fluorescent protein in its native genomic locus. Each strain also expressed Sad1p–red fluorescent protein (RFP) or Sad1p–cyan fluorescent protein (CFP) to mark spindle pole bodies (SPBs), which we used to establish a time course within the cell cycle in which SPB separation at the onset of anaphase marks time zero (Wu *et al.*, 2003). Events that occur before SPB separation have negative time values, and events after SPB separation have a positive time values.

Blt1p concentrated in cortical nodes along with kinase Cdr2p–monomeric enhanced green fluorescent protein (mEGFP) and anillin-like Mid1p–monomeric yellow fluorescent protein (mYFP) during interphase (Figure 1, –90 ±10 to –15 ± 4 min; Wu *et al.*, 2003; Moseley *et al.*, 2009; Saha and Pollard, 2012). Cdr2p disappeared from nodes early in mitosis (+6 ± 2 min), but Blt1p and Mid1p remained in nodes and were joined by formin Cdc12p-mYFP (0 ± 3 min) and F-BAR protein Cdc15p-mYFP (–5 ± 2 min) before being incorporated into fully formed contractile rings (+25 ± 3 min; Wu *et al.*, 2003; Moseley *et al.*, 2009). Mid1p-mYFP disappeared from the contractile ring before the onset of ring constriction (+28 ± 3 min), but Blt1p-mEGFP remained in the ring with Cdc12p-mYFP and Cdc15p-mYFP until the completion of ring constriction (+62 ± 6 min; Wu *et al.*, 2003). The majority of Blt1p-mEGFP remained at the division site along with Bgs1p-mEGFP after completion of septation (+68 ± 5 min; Cortes *et al.*, 2002), before relocalizing to cortical nodes at the middle of the cell (+90 ± 10 min).

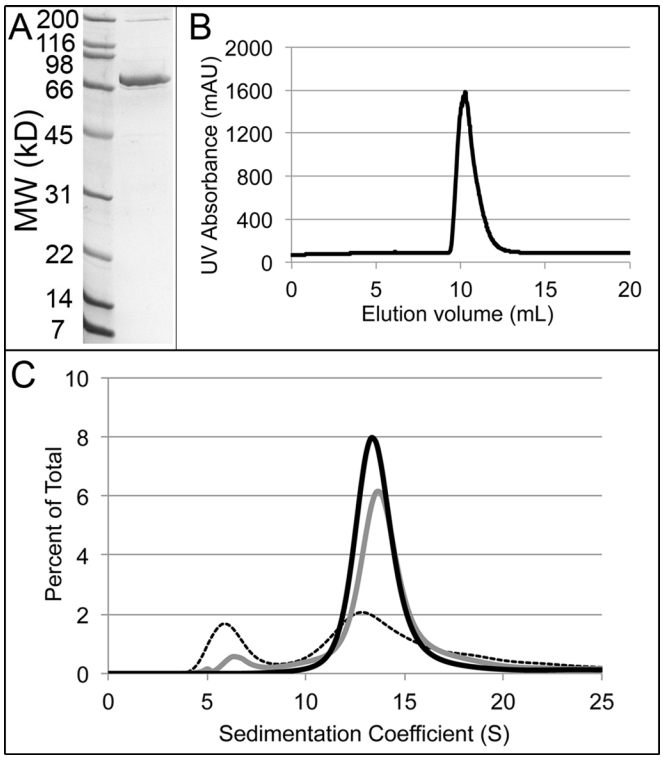

FIGURE 2: Native Blt1p forms homotetramers. (A) SDS–PAGE of purified recombinant Blt1p-hexahistidine stained with Coomassie blue with standards in the left lane. (B) Elution of purified Blt1p in 20 mM Tris, pH 8.0, 20 mM NaCl, 0.5 mM EDTA, and 1 mM DTT from a calibrated Superdex 200 gel filtration column followed by ultraviolet absorption. (C) Distributions of sedimentation coefficients determined by sedimentation velocity analytical ultracentrifugation at 20°C, assuming a continuous *c*(*S*) distribution. Conditions are the same as B. Three concentrations of Blt1p: dashed, 0.1 μM; gray, 1.0 μM; and black, 10 μM.

Blt1p purification and characterization

We purified full-length Blt1p fused to a hexahistidine tag from *Escherichia coli* and evaluated its hydrodynamic properties to provide a physical context for our analysis of its contributions to cytokinesis. We used affinity chromatography on nickel-nitriloacetic acid (Ni-NTA beads), followed by ion-exchange and size-exclusion chromatography. Consistent with the molecular weight calculated from its amino acid sequence (78.1 kDa), purified Blt1p migrated at ~70 kDa on SDS–PAGE (Figure 2A). Although the C-terminal 75 residues of Blt1p are postulated to interact with membrane lipids (Guzman-Vendrell *et al.*, 2013), full-length recombinant Blt1p was soluble between 4 and 25°C at neutral pH in salt concentrations ranging from 10 to 300 mM.

Hydrodynamic analysis showed that native Blt1p is a tetramer in equilibrium with its 78-kDa subunits. Purified Blt1p eluted from a calibrated Superdex 200 column with a partition coefficient of 0.145, corresponding to a Stokes radius of 68 Å and a diffusion coefficient of 3.25×10^{-8} cm^2/s (Figure 2B and Table 1). This Stokes radius is much larger than that of serum albumin (35 Å), which has a subunit molecular weight (66 kDa) similar to that of Blt1p (Erickson, 2009). This suggested that Blt1p forms homo-oligomers or is highly asymmetric. Sedimentation velocity analytical ultracentrifugation showed that purified Blt1p is a hydrodynamically well-behaved oligomer. At 10 μM virtually all Blt1p sedimented at 13.6 S, whereas at low concentrations (0.1 μM) an additional, more slowly sedimenting species was present at 6.3 S (Figure 2C). We also determined the diffusion coefficient (*D*) for both species from boundary spreading of the sedimenting protein (Table 1). The *S* and *D* values gave molecular weights of ~75 kDa for the 6-S species, consistent with the size of the Blt1p monomer, and ~343 kDa for the 14-S species (Figure 2C and Table 1), indicating that Blt1p forms homotetramers. The frictional coefficient of 1.3 indicates that the Blt1p tetramer is a slightly asymmetric molecule.

Blt1p ensures proper timing for onset of contractile ring constriction

Careful quantitative analysis revealed no differences in contractile ring assembly between wild-type and *blt1Δ* cells in spite of the prominence of Blt1p in interphase and cytokinesis nodes. Supplemental Figures S1 and S2 document that myosin-II mEGFP-Myo2p, unconventional myosin-II Myp2p-mYFP, and Cdc15p-mEGFP each appeared in nodes and contractile rings at the same times in wild-type and *blt1Δ* cells. Furthermore, the numbers of these proteins in rings and the time required for ring formation were normal in *blt1Δ* cells (see Supplemental Results). Measurements of Rlc1p, the regulatory light chain for both type II myosins, Myo2p and Myp2p (Le Goff *et al.*, 2000; Naqvi *et al.*, 2000), showed that it appears in the contractile ring in two waves, the first consisting of ~4000 molecules, associated with Myo2p (Supplemental Figures S1F and S2B), and the second consisting of ~2000 molecules, associated with Myp2p (Supplemental Figure S2, B and E) in both wild-type and *blt1Δ* cells.

The first cytokinesis defect to appear in *blt1Δ* cells during the cell cycle was a 10-min delay in the onset of contractile ring constriction to time 38 ± 5 min (Figure 3, A and B). Ring constriction and septation took the normal times in *blt1Δ* cells, so completion of septation and separation of daughter cells were delayed 11 min from an average of 68 ± 5 min in wild-type cells to 79 ± 5 min in *blt1Δ* cells (Figure 3B). The timing of anaphase A, anaphase B, and telophase was normal in *blt1Δ* cells (Supplemental Figure S3).

Genetic and physical interactions of Blt1p with SIN components Mid1p and Sid2p

Because we found no evidence that the defect in the onset of contractile ring constriction in *blt1Δ* cells was due to mislocalization of

A. Gel filtration				
	Stokes radius (Å)	**Diffusion coefficient (cm^2/s)**		
Blt1p oligomer	68	3.3×10^{-8}		
B. Sedimentation velocity, analytical ultracentrifugation				
	Sedimentation coefficient (s^{-1})	**Diffusion coefficient (cm^2/s)**	**Calculated molecular weight (g/mol)**	**f/f_0**
Blt1p monomer	6.3×10^{-13}	7.5×10^{-8}	75,457	1.2
Blt1p oligomer	13.6×10^{-13}	3.6×10^{-8}	343,245	1.3

TABLE 1: Hydrodynamic properties of Blt1p-hexahistidine.

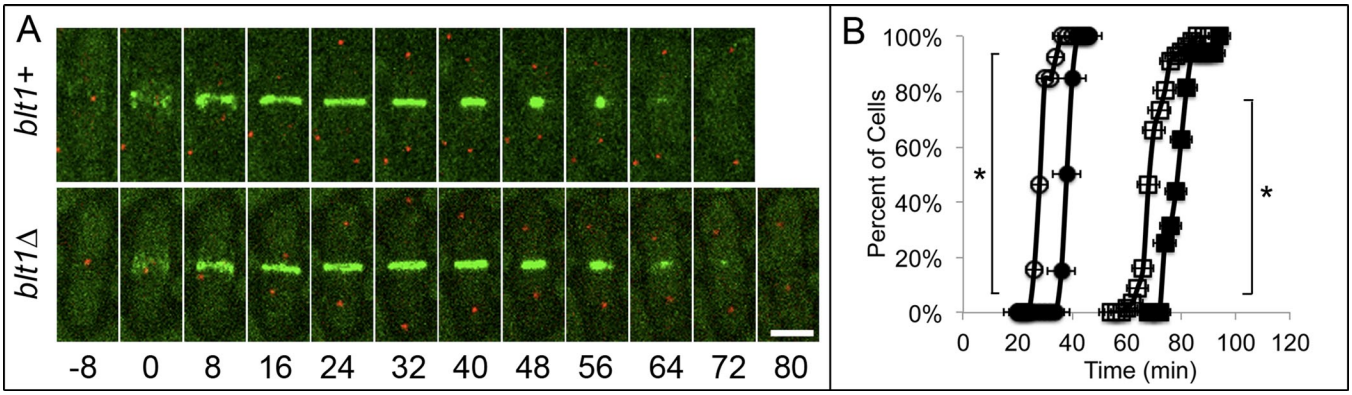

FIGURE 3: The onset and completion of contractile ring constriction are delayed in *blt1Δ* cells relative to wild-type cells. Times are in minutes, with spindle pole body separation defined as time zero. (A) Time series of fluorescence micrographs at 8-min intervals of (top) wild-type *blt1⁺* cells and (bottom) *blt1Δ* cells expressing Rlc1p-mEGFP (green) to mark nodes and contractile rings and Sad1p-RFP (red) to mark spindle pole bodies. (B) Time courses of the accumulation of cells ±1 SD (○, ●) beginning contractile ring constriction and (□, ■) completing septation. Open symbols are 22 wild-type cells, and filled symbols are 27 *blt1Δ* cells expressing Rlc1p-mEGFP. Asterisks indicate time points at which the mean values of the two cell types differed with $p < 0.0001$. Scale bar, 5 μm.

cytokinesis node proteins, we sought other proteins that interact with Blt1p by screening for decreased viability at 25, 30, or 36°C of double mutants of *blt1Δ* with mutations of other cytokinesis genes in strains with the same auxotrophic markers (Table 2 and Supplemental Figure S4). Our quantitative analysis identified synthetic interactions between *blt1Δ* and genes for multiple components of the SIN, including the terminal components of the signaling pathway, *mob1⁺* and *sid2⁺* (Figure 4A). The NDR-family kinase Sid2p and its accessory protein Mob1p regulate contractile ring constriction and septation (Sparks *et al.*, 1999; Hou *et al.*, 2000; Salimova *et al.*,

		Relative percentage growth[a]					
		25°C		30°C		36°C	
***S. pombe* mutation**	**Generic name**	**Mutant**	**+ *blt1Δ***	**Mutant**	**+ *blt1Δ***	**Mutant**	**+ *blt1Δ***
Wild type		100	96 ± 5	100	85 ± 10	100	81 ± 6
cdc11-19	SIN scaffold protein	95 ± 9	93 ± 3	97 ± 4	88 ± 10	22 ± 11	13 ± 9
cdc14-118	SIN component	80 ± 5	60 ± 16	62 ± 8	24 ± 11	0 ± 0	0 ± 0
cdc15-127	F-BAR protein	96 ± 3	91 ± 4	90 ± 5	81 ± 23	12 ± 5	8 ± 7
cdc16-116	SIN GAP	88 ± 8	58 ± 14	11 ± 3	2 ± 1	0 ± 0	0 ± 0
cdc2-M26	Cyclin-dependent kinase 1	77 ± 5	71 ± 7	67 ± 2	58 ± 7	61 ± 9	52 ± 6
cdc25-22	Phosphatase	87 ± 7	81 ± 9	60 ± 10	31 ± 15	9 ± 2	6 ± 4
cdc3-6	Profilin	85 ± 12	70 ± 10	65 ± 2	52 ± 15	1 ± 1	1 ± 2
cdc4-8	Myosin-II light chain	91 ± 7	82 ± 11	77 ± 9	56 ±15	72 ± 11	51 ± 13
cdc7-24	SIN kinase	72 ± 14	65 ± 6	53 ± 12	34 ± 13	0 ± 0	0 ± 0
cdc8-27	Tropomyosin	95 ± 6	77 ± 12	86 ± 5	56 ± 6	0 ± 0	0 ± 0
cps1-119	(1,3)β-D-Glucan synthase	90 ± 3	83 ± 8	60 ± 3	53 ± 11	2 ± 1	1 ± 1
mid1Δ	Anillin	33 ± 11	17 ± 7	36 ± 3	15 ± 7	15 ± 8	10 ± 6
mob1-R4	SIN regulatory subunit	45 ± 5	25 ± 14	21 ± 7	11 ± 6	0 ± 0	0 ± 0
myo2-E1	Myosin-II heavy chain	83 ± 12	67 ± 8	51 ± 9	30 ± 11	2 ± 1	3 ± 3
plo1-24C	Polo kinase	79 ± 6	65 ± 4	78 ± 8	49 ± 9	12 ± 6	12 ± 8
rng2-D5	IQGAP	93 ± 8	88 ± 7	80 ± 7	70 ± 4	15 ± 6	11 ± 9
sid1-125	SIN kinase	57 ± 12	55 ± 9	41 ± 8	16 ± 10	0 ± 0	0 ± 0
sid2-250	SIN Ndr-family kinase	63 ± 6	40 ± 19	11 ± 8	6 ± 4	0 ± 0	0 ± 0
sid4-A1	SIN scaffold protein	72 ± 11	21 ± 9	1 ± 2	2 ± 2	0 ± 0	0 ± 0
spg1-106	SIN GTPase	30 ± 10	13 ± 12	11 ± 3	5 ± 2	0 ± 1	0 ± 0

[a]Percentage growth shown on plates at 25°C for 48 h, 30°C for 36 h, or 36°C for 36 h.

TABLE 2: Genetic interactions with *blt1Δ*.

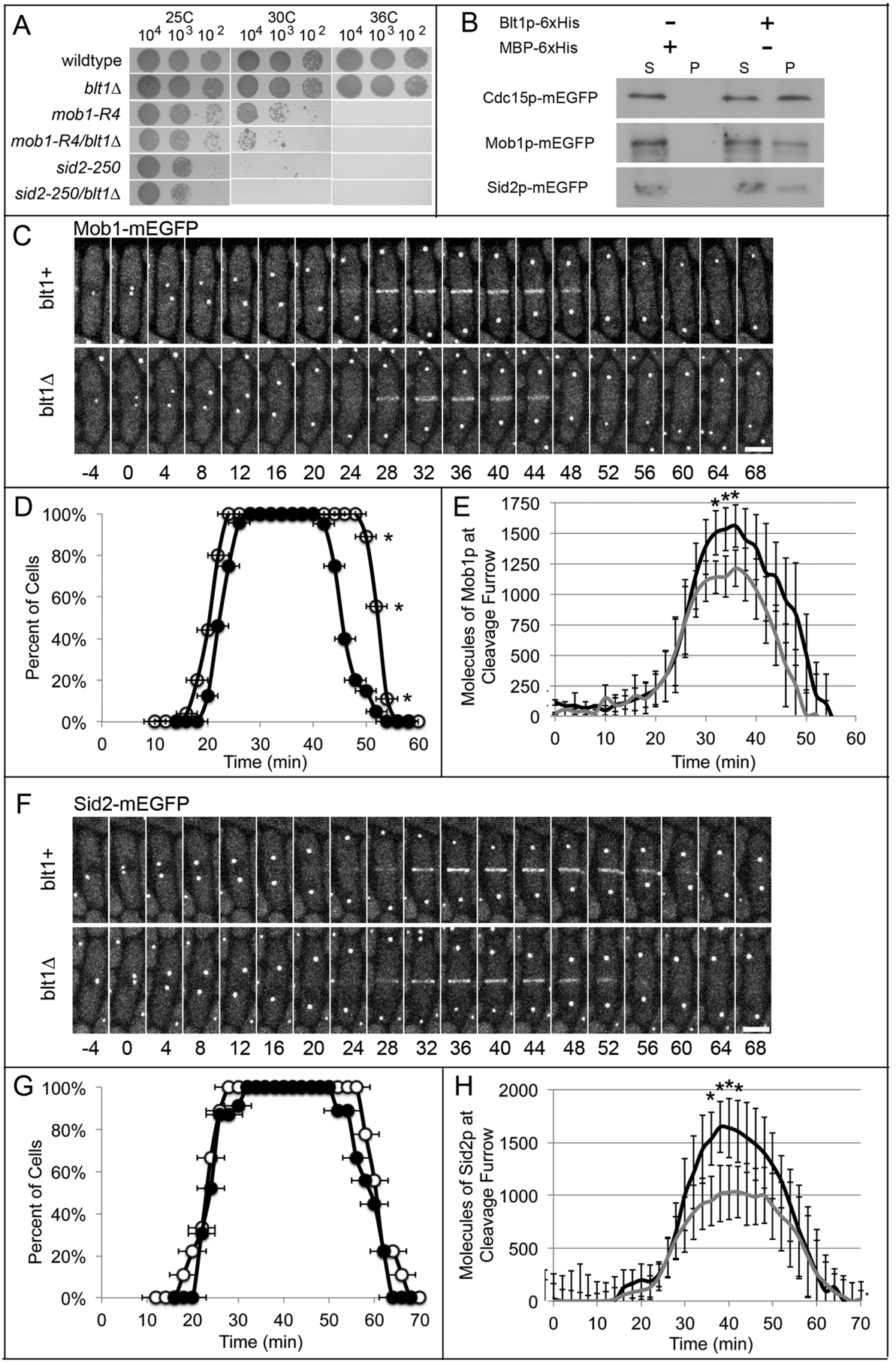
A
25C
30C
36C
10^4 10^3 10^2
wildtype
blt1Δ
mob1-R4
mob1-R4/blt1Δ
sid2-250
sid2-250/blt1Δ
B
Blt1p-6xHis
MBP-6xHis
S P S P
Cdc15p-mEGFP
Mob1p-mEGFP
Sid2p-mEGFP
C
Mob1-mEGFP
blt1+
blt1Δ
-4 0 4 8 12 16 20 24 28 32 36 40 44 48 52 56 60 64 68
D
Percent of Cells
Time (min)
E
Molecules of Mob1p at Cleavage Furrow
Time (min)
F
Sid2-mEGFP
blt1+
blt1Δ
-4 0 4 8 12 16 20 24 28 32 36 40 44 48 52 56 60 64 68
G
Percent of Cells
Time (min)
H
Molecules of Sid2p at Cleavage Furrow
Time (min)

2000). The growth defects of point mutants *mob1-R4* and *sid2-250* were more severe when combined with *blt1Δ* at both 25 and 30°C (Figure 4A and Supplemental Figure S4).

Pull-down assays confirmed physical interactions between Blt1p and these SIN components; Blt1p pulled down from lysates 42% of Mob1p-mEGFP and 22% of Sid2p-mEGFP, as well as 23% of Cdc15p-mEGFP (Figure 4B), as described previously (Moseley *et al.*, 2009). Ni-NTA beads lacking Blt1p did not pull down any of these fluorescent fusion proteins from lysates (Figure 4B). Mob1p and Sid2p interact with each other, and both are essential, so we could not determine whether Blt1p interacts with just one or both of Mob1p and Sid2p.

Timely localization of Mob1p and Sid2p to the contractile ring depends on Bl1p

The presence of Blt1p influenced the relocation of Mob1p-mEGFP and Sid2p-mEGFP from SPBs to the contractile ring during cytokinesis. Mob1p and Sid2p concentrate in SPBs throughout the cell cycle, but unlike other SIN proteins, both move to the contractile ring during mitosis (Sparks *et al.*, 1999; Hou *et al.*, 2000, 2004; Salimova *et al.*, 2000; McCormick *et al.*, 2013). In wild-type cells, Mob1p appeared around the equator at time +21 ± 2 min, increased to a peak average of 1500 ± 180 molecules at +36 min, and departed by +53 ± 2 min (Figure 4, C–E). In *blt1Δ* cells, Mob1p arrived at the equator at time +24 ± 2 min and initially accumulated at the same rate as in wild-type cells but then slowed and peaked at 1200 ± 170 molecules at +36 min and departed earlier at +46 ± 2 min (Figure 4, C–E). Ring constriction began in wild-type cells at +28 min, when 1200 ± 270 molecules of Mob1p were present in the ring, but was delayed until +38 min in *blt1Δ* cells, when the ring contained an average of 1200 ± 210 molecules of Mob1p (Figure 4E).

Similar to Mob1p, Sid2p appeared in the contractile ring at about the same time in wild-type cells (+23 ± 2 min; departing by +62 ± 3 min) and *blt1Δ* cells (+26 ± 2 min; departing by +58 ± 3 min; Figure 4, F and G), but the peak number of Sid2p molecules was much lower (1000 ± 240 at +40 min) in *blt1Δ* cells than in wild-type cells (1700 ± 280 at +40 min; Figure 4H). Rings in wild-type cells accumulated 1000 ± 270 molecules of Sid2p at the time they began to constrict at +28 min, whereas rings in *blt1Δ* cells did not begin to constrict until +38 min with an average of 1000 ± 270 molecules of Sid2p (Figure 4H). Wild-type and *blt1Δ* cells have the same total number of Mob1p or Sid2p molecules (Supplemental Figure S5, A and B). Thus contractile rings in both wild-type and *blt1Δ* cells begin to constrict when they accumulate ~1000 active Sid2p/Mob1p kinase complexes. This suggests that a threshold level of kinase activity might trigger constriction.

To test this hypothesis, we varied the total numbers of Mob1p-mYFP and Sid2p-mYFP in cells using the *3nmt* promoter and its repressor, thiamine, to control their expression. Without thiamine, the *3nmt* promoter produced wild-type levels of both proteins, but growth in liquid culture for 10 h with 15 μM thiamine modestly reduced the total number of Mob1p-mYFP from 35,100 ± 600 to 23,300 ± 500 molecules/cell and the total number of Sid2p-mYFP from 31,300 ± 2000 to 21,500 ± 1100 molecules/cell (Supplemental Figure S5, A, B, E, and F). This mild repression of either Sid2p or Mob1p had no effect on recruitment of Mob1p-YFP or Sid2p-mYFP to SPBs or the timing of anaphase A, anaphase B, or telophase (Supplemental Figure S7, A–D). This is expected from the micromolar cytoplasmic concentrations of Mob1p and Sid2p and the high affinity of their receptor, Cdc11p, on SPBs (McCormick *et al.*, 2013). However, mild depletion of Mob1p and Sid2p delayed ring constriction 7–8 min to the time when the rings contained 1000 molecules of Mob1p-mYFP and Sid2p-mYFP, the same numbers at the onset of constriction in unrepressed cells (Supplemental Figure S6, D and F). This indicates that the unknown contractile ring receptor for Mob1p/Sid2p has a lower affinity than Cdc11p in SPBs. Thus, under three different conditions, contractile rings began to constrict when ~1000 molecules of Sid2p/Mob1p accumulated in the ring.

Gef2p is not required for localization of Mob1p and Sid2p to the contractile ring

Because localization of Gef2p to interphase nodes and to the cleavage site depends on Blt1p (Moseley *et al.*, 2009; Ye *et al.*, 2012; Jourdain *et al.*, 2013), and since Gef2p is proposed to regulate the SIN (Ye *et al.*, 2012), we expected that a shortage of equatorial Gef2p in the *blt1Δ* cells might explain the slow accumulation of Mob1p and Sid2p in rings. Consistent with previous studies, contractile rings in *blt1Δ* cells accumulated fewer molecules of Gef2p (peak of 480 ± 150 molecules at +36 min) than wild-type cells (peak of 1300 ± 300 molecules at +40 min) (Supplemental Figure S8).

Nevertheless, Mob1p and Sid2p both accumulated normally in rings of *gef2Δ* cells. The average times of Mob1p appearance (+21 ± 2 min wild type; +20 ± 3 min *gef2Δ*), peak numbers of Mob1p molecules at the cleavage site (1600 ± 200 wild type; 1300 ± 300 *gef2Δ*), and leaving times (+53 ± 2 min wild type; +55 ± 3 min *gef2Δ*) did not differ significantly in the two strains

FIGURE 4: Blt1p contributes to Mob1p and Sid2p localization at the division site. Times are in minutes, with spindle pole body separation at time zero. (A) Growth for 72 h at 25, 30, or 36°C on YE5S agar plates of 5-μl aliquots of 10-fold serial dilutions of wild-type cells and mutant strains *blt1Δ*, *mob1-R4*, *mob1-R4/blt1Δ*, *sid2-250*, and *sid2-250/blt1Δ*. (B) Binding of Cdc15p-mEGFP, Mob1p-mEGFP, or Sid2p-mEGFP in *S. pombe* lysates to Blt1p-hexahistidine immobilized on beads. Western blots using antibodies to GFP show the distributions of these proteins between the (S) supernatant and (P) washed pellet fractions. (C) Time series of fluorescence micrographs at 4-min intervals of (top) wild-type *blt1⁺* cells and (bottom) *blt1Δ* cells expressing Mob1p-mEGFP (white). Scale bar, 5 μm. (D) Time courses of the localization of Mob1p-mEGFP ±1 SD in a band/ring at the division site in (○) 37 wild-type cells and (●) 39 *blt1Δ* cells. Asterisks indicate time points at which the mean values of the two cell types differed with $p < 0.0008$. (E) Time course of the mean number of Mob1p-mEGFP molecules ± 1 SD localized at the division site in 31 wild-type cells (black line) and 29 *blt1Δ* cells (gray line). Asterisks indicate time points at which the mean values of the two cell types differed with $p < 0.0001$. (F) Time series of fluorescence micrographs at 4-min intervals of (top) wild-type *blt1+* cells and (bottom) *blt1Δ* cells expressing Sid2p-mEGFP (white). Scale bar, 5 μm. (G) Time courses of the localization of Sid2p ±1 SD at the division site in (○) 24 wild-type cells and (●) 21 *blt1Δ* cells. None of these mean values differs significantly between the strains. (H) Time course of the mean number of Sid2p molecules ±1 SD localized at the division site in 24 wild-type cells (black line) and 21 *blt1Δ* cells (gray line). Asterisks indicate time points at which the mean values of the two cell types differed with $p < 0.0002$.

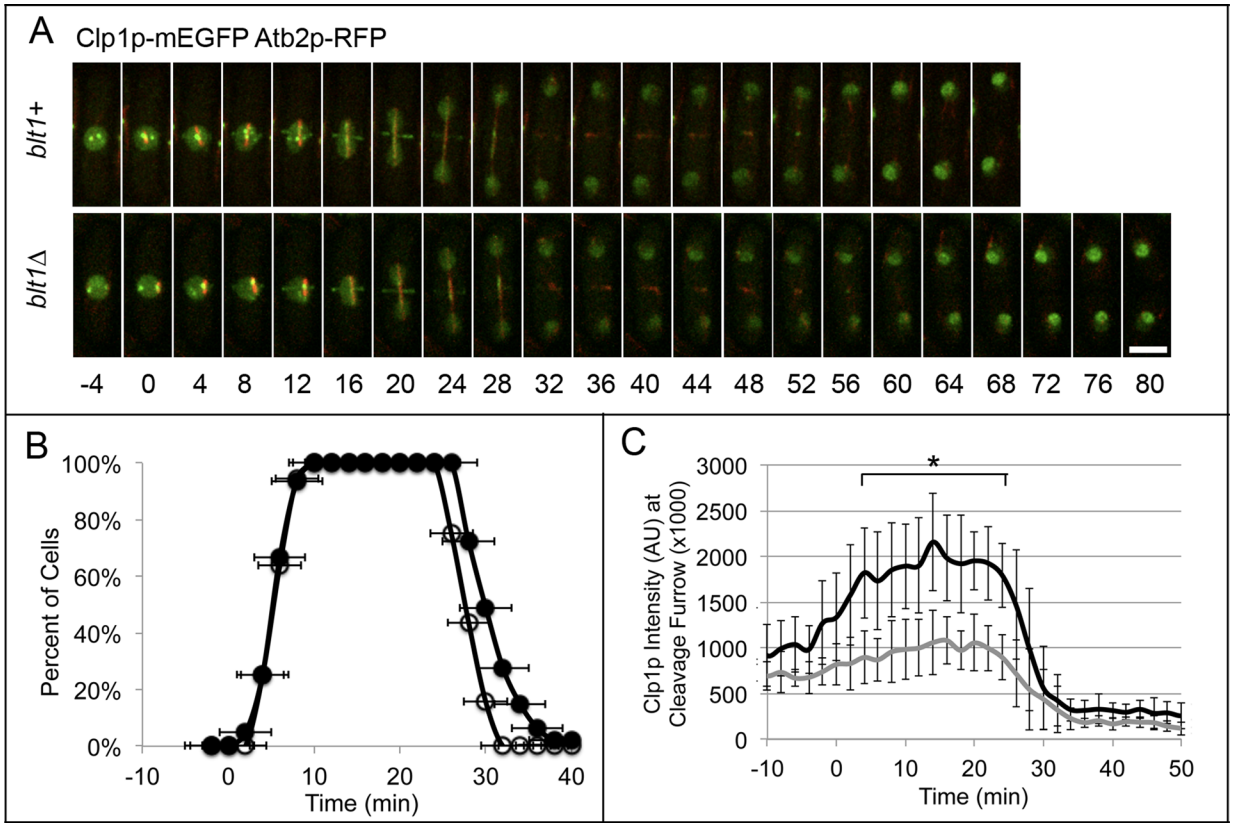

FIGURE 5: Clp1p localization at the cleavage site is decreased in *blt1Δ* cells. Times are in minutes, with spindle pole body separation at time zero. (A) Time series of fluorescence micrographs at 4-min intervals of wild-type (*blt1*$^+$, top) or *blt1Δ* (bottom) cells expressing Clp1p-mEGFP (green) and α-tubulin Atb2p-RFP (red). Arrows indicate Clp1p-mEGFP at the cleavage site. Scale bar, 5 μm. (B) Time courses of the accumulation of cells with Clp1p-mEGFP ±1 SD in a ring around the equator in (○) 36 wild-type cells and (●) 47 *blt1Δ* cells. Asterisks indicate time points at which the mean values of the two cell types differed with $p < 0.04$. (C) Time course of the mean number of Clp1p-mEGFP molecules ±1 SD localized at the site of cleavage in 23 wild-type (black line) and 23 *blt1Δ* (gray line) cells. Asterisks indicate time points at which the mean values of the two cell types differed with $p < 0.0001$.

(Supplemental Figure S9, A–C). Similarly, the average times of Sid2p appearance (+23 ± 3 min wild type; +23 ± 2 min *gef2Δ*), peak numbers of Sid2p molecules at the cleavage furrow (1700 ± 300 wild type; 1400 ± 200 *gef2Δ*), and leaving times (+62 ± 3 min wild type; +60 ± 4 min *gef2Δ*) were indistinguishable (Supplemental Figure S10, A–C). Therefore reduced equatorial Gef2p is unlikely to explain the slow accumulation of Mob1p and Sid2p in rings of *blt1Δ* cells.

The absence of Blt1p reduces Clp1p in the contractile ring

The Cdc14-family phosphatase Clp1p is a key regulator of cytokinesis and mitotic exit in fission yeast (Cueille *et al.*, 2001; Trautmann *et al.*, 2001; Esteban *et al.*, 2004; Wolfe and Gould, 2004). Because retention of Clp1p in the cytoplasm during cytokinesis depends on phosphorylation by Sid2p (Chen *et al.*, 2008), we investigated whether the slow accumulation of Sid2p in contractile rings of *blt1Δ* cells might compromise the localization of Clp1p to the cleavage site. Wild-type and *blt1Δ* cells had the same total number of Clp1p molecules (Supplemental Figure S5C).

As anticipated, the fluorescence intensity of Clp1p-mEGFP around the equator was much lower in the absence of Blt1p (Figure 5C), although the timing of its appearance in the ring was normal (Figure 5B). (We could not determine the exact number of Clp1p molecules in the ring due to the fluorescence of Clp1p-mEGFP in the nucleus and mitotic spindle.) Clp1p-mEGFP localized to an equatorial ring at time +6 ± 2 min and remained until +29 ± 2 min in wild-type cells and appeared in the ring from time +6 ± 2 min until +32 ± 5 min in *blt1Δ* cells (Figure 5, A and B).

The absence of Blt1p delays the synthesis of the primary septum in the cleavage furrow

Because the accumulation of (1,3)β-D-glucan synthase Bgs1p/Cps1p at the cleavage site depends on SIN activity (Le Goff *et al.*, 1999; Liu *et al.*, 1999, 2000; Cortes *et al.*, 2002), we investigated the behavior of Bgs1p in *blt1Δ* cells. Wild-type and *blt1Δ* cells have the same total number of molecules of this transmembrane enzyme that synthesizes the primary septum (Supplemental Figure S5D), and Bgs1p-mEGFP began to accumulate around the equator at the same time in wild-type (+16 ± 2 min) and *blt1Δ* (+17 ± 1 min) cells. Nevertheless, cells without Blt1p had four defects in the regulation of Bgs1p. First, the concentration of Bgs1p into a narrow ring was delayed from +27 ± 2 min in wild-type cells until +32 ± 2 min in *blt1Δ* cells (Figure 6, A and B). Second, the peak number of Bgs1p molecules at the cleavage site was reduced from 11,800 ± 2600 molecules at +42 min in wild-type cells to 8000 ± 1200 molecules at +64 min in *blt1Δ* cells (Figure 6D). Third, constriction of contractile rings was delayed from +28 min when wild-type cells accumulated 8200 ± 1200 molecules of Bgs1p at the cleavage site to +38 min in *blt1Δ* cells when 7700 ± 600 molecules of Bgs1p-mEGFP

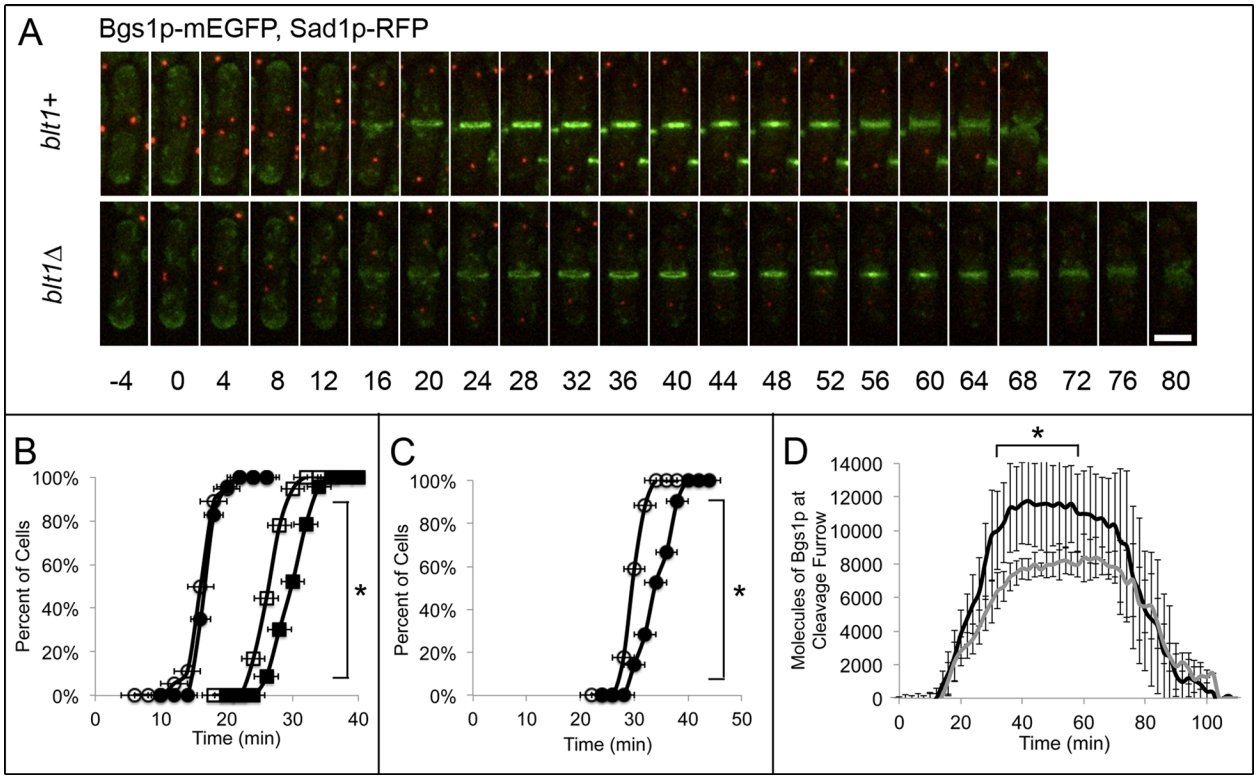

FIGURE 6: Primary septum assembly is delayed in *blt1Δ* mutants. Times are in minutes, with spindle pole body separation at time zero. (A) Time series of fluorescence micrographs at 4-min intervals of wild-type (*blt1*$^+$, top) or *blt1Δ* (bottom) cells expressing Bgs1p-mEGFP (green) and Sad1p-RFP (red). (B, C) Comparisons of wild-type (open symbols) and *blt1Δ* (filled symbols) cells. (B) Time courses of (○, ●) the accumulation of cells with diffuse localization of Bgs1p-mEGFP ±1 SD around the equator (12 min in the *blt1*$^+$ cell in A) and (□, ■) accumulation of cells with Bgs1p-mEGFP ±1 SD condensed into a ring at the site of primary septum formation (as shown in the *blt1*$^+$ cell in A at 24 min) in 33 wild-type cells and 36 *blt1Δ* cells. Asterisks indicate time points at which the mean values of the two cell types differed with $p < 0.0003$. (C) Time courses of the onset of primary septum assembly ±1 SD in (○) 33 wild-type and (●) 36 *blt1Δ* cells. Asterisks indicate time points at which the mean values of the two cell types differed with $p < 0.0001$. (D) Time course of the mean number ±1 SD of Bgs1p-mEGFP molecules at the cleavage furrow in 20 wild-type cells (black line) and 21 *blt1Δ* cells (gray line). Asterisks indicate time points at which the mean values of the two cell types differed with $p < 0.0001$. Scale bar, 5 μm.

were present at the cleavage site (Figure 6D). Fourth, completion of the septum with the formation of a disk of Bgs1p-mEGFP (Cortes *et al.*, 2002) was delayed from +50 ± 3 min in wild-type cells to +57 ± 3 min in *blt1Δ* cells (Figure 6C).

Although contractile rings assembled normally in the middle of wild-type and *blt1Δ* cells, three times more rings moved at least 0.5 μm laterally from the cell equator in *blt1Δ* than in wild-type cells, and many also tilted obliquely to the long axis (Supplemental Figure S11, A–C). Contractile rings slid in *blt1Δ* cells during the delay in the accumulation of Bgs1p-mEGFP, as observed under other conditions when Bgs1p arrived late at the cleavage site relative to the normal onset of constriction (Liu *et al.*, 1999; Pardo and Nurse, 2003; Huang *et al.*, 2008; Roberts-Galbraith *et al.*, 2010).

DISCUSSION

We find that Blt1p is required for proper timing of contractile ring constriction and the normal rates of accumulation of the SIN kinase complex Sid2p/Mob1p, phosphatase Clp1p, and β-glucan synthase Bgs1p at the division site. Given previous work (Le Goff *et al.*, 1999; Liu *et al.*, 1999, 2000; Cortes *et al.*, 2002; Chen *et al.*, 2008), the slow recruitment of Sid2p/Mob1p likely explains the slow accumulation of Clp1p and Bgs1p, which in turn contributes to the onset of ring constriction and septum formation.

Blt1p is not required for contractile ring assembly

The presence of Blt1p in interphase nodes suggested that it might recruit other proteins to cytokinesis nodes or contractile rings, but the only example we found was the known dependence of Gef2p localization in interphase nodes on Blt1p (Moseley *et al.*, 2009; Ye *et al.*, 2012; Guzman-Vendrell *et al.*, 2013; Jourdain *et al.*, 2013). We measured a 60% decrease in Gef2p in cytokinesis nodes and contractile rings in *blt1Δ* cells but found that Gef2p is not required for normal rates of accumulation or disappearance of Mob1p/Sid2p in contractile rings. Although Gef2p disappears earlier than normal from the division site in *blt1Δ* cells, cells without Gef2p divide normally (Ye *et al.*, 2012). In the absence of Blt1p, Mid1p mediates the localization of Gef2p to cytokinesis nodes and the contractile ring (Guzman-Vendrell *et al.*, 2013), but it is unclear what retains Gef2p at the ring after Mid1p departs in *blt1Δ* cells.

Our quantitative measurements showed that Blt1p is not required to recruit myosin-II (Myo2p and Rlc1p) or the F-BAR protein Cdc15p to cytokinesis nodes or the contractile ring or unconventional myosin Myp2p to the contractile ring, in spite of many other mutations causing delays in the appearance of these proteins (Fankhauser *et al.*, 1995; Bezanilla *et al.*, 1997; Mulvihill and Hyams, 2003; Coffman *et al.*, 2009; Sladewski *et al.*, 2009; Roberts-Galbraith, 2010). We found that contractile rings form with precisely normal

timing in *blt1Δ* cells, confirming previous qualitative observations (Moseley *et al.*, 2009; Ye *et al.*, 2012; Guzman-Vendrell *et al.*, 2013; Jourdain *et al.*, 2013). Furthermore, rings in *blt1Δ* cells constricted at a normal rate in spite of a 10-min delay in the onset of constriction. This shows that the cytokinesis defect in *blt1Δ* cells is confined to the events that initiate constriction.

Blt1p recruits Mob1p and Sid2p to the contractile ring and promotes ring constriction

Our mutant screen revealed strong genetic interactions between *blt1Δ* and mutations in genes (*cdc25*$^{+}$ and *mid1*$^{+}$) that function in interphase or at the G2/M transition (Paoletti and Chang, 2000; Martin and Berthelot-Grosjean, 2009; Moseley *et al.*, 2009), but the most extensive interactions were with genes for SIN components that lead to phosphorylation of Sid2p (Sparks *et al.*, 1999; Hou *et al.*, 2004). The Sid2p/Mob1p complex carries the SIN signal from the SPBs to the contractile ring (Sparks *et al.*, 1999; Chen *et al.*, 2008). Mutations of SIN pathway genes compromise maturation of the contractile ring, which can delay the onset of constriction (Hachet and Simanis, 2008).

Our measurements indicate that Blt1p is required for the timely recruitment and retention of Sid2p and Mob1p at the division site (Figure 4B). The kinase complex may interact directly with Blt1p, but the large Blt1p tetramer may also function as a scaffold and contribute to the architecture of nodes and the ability of other receptors to bind Sid2p/Mob1p. Previous work implicated microtubules in localizing Mob1p and Sid2p to the division plane (Sparks *et al.*, 1999), but the mechanisms retaining these proteins at the contractile ring were unknown. In both wild-type and *blt1Δ* cells, contractile rings begin to constrict when ~1000 molecules of Sid2p/Mob1p accumulate in the ring. Contractile rings in cells without Blt1p or depleted of Mob1p or Sid2p recruit Sid2p/Mob1p complexes more slowly and accumulate 1000 complexes ~10 min later than wild-type cells. Mutations that reduced Sid2p/Mob1p complex activation also extend the time required to recruit Sid2p/Mob complexes, possibly accounting for the growth defects in *blt1Δ* mutants with a SIN mutation (Table 2 and Supplemental Figure S4).

Blt1p must cooperate with other proteins to recruit and retain Sid2p and Mob1p in contractile rings, since both proteins appear in rings in reduced numbers in *blt1Δ* cells. Our results indicate that putative Rho-GEF Gef2p is unlikely to be this second receptor, and our genetic screen (Table 2) did not provide other candidates. In fact, Gef2p might antagonize Blt1p in regulating SIN activation, given that the *gef2Δ* mutation partially suppresses growth defects of the mutations *sid2-250* and the Sid2p/Mob1p receptor *cdc11-136* (Ye *et al.*, 2012).

We propose that the onset of contractile ring constriction depends on a threshold level of Sid2p/Mob1p in the ring to phosphorylate the Cdc14-like phosphatase Clp1p. This hypothesis offers an explanation for why contractile rings in *blt1Δ* cells with decreased Sid2p also have half the normal Clp1p. Phosphorylation of Clp1p promotes its retention in the cytoplasm and its concentration in the contractile ring, so with defects in SIN signaling, Clp1p is targeted back to the nucleus, resulting in cytokinesis defects (Trautmann *et al.*, 2001; Mishra *et al.*, 2004; Chen *et al.*, 2008).

At the division plane, Clp1p dephosphorylates Cdc15p, contributing to formation and constriction of the contractile ring (Clifford *et al.*, 2008; Roberts-Galbraith *et al.*, 2010). Low numbers of Cdc15p in contractile rings of *sid2* mutants (Hachet and Simanis, 2008) are presumably due to a failure to stabilize Clp1p at the division plane and a corresponding decrease in Cdc15p dephosphorylation. We found normal numbers of Cdc15p molecules in contractile rings of *blt1Δ* mutants, showing that half the number of Clp1p at the division site provides enough enzyme activity to retain Cdc15p at the contractile ring, although not enough activity to avoid a delay in the onset of ring constriction.

Blt1p contributes to primary septum formation and division plane stability

The absence of Blt1p delays recruitment of Bgs1p to the cleavage furrow and the onset of primary septum synthesis, since these processes depend on output from SIN (Le Goff *et al.*, 1999; Liu *et al.*, 1999; Cortes *et al.*, 2002; Jin *et al.*, 2006) and cell wall synthesis contributes to ingression of the cleavage furrow (Liu *et al.*, 1999; Proctor *et al.*, 2012). In both wild-type and *blt1Δ* cells, contractile ring constriction and primary septum synthesis begin at the point where ~8000 molecules of Bgs1p accumulate at the division plane, but reaching this number of Bgs1p molecules takes 10 min longer without Blt1p. During this delay in the initiation of primary septum synthesis and ring constriction, contractile rings may slide away from the cell equator and displace the division plane, as observed under other conditions that disrupt assembly of the primary septum (Liu *et al.*, 1999; Pardo and Nurse, 2003; Huang *et al.*, 2008). Although the direct link between the Mob1p/Sid2p and Bgs1p has not been identified, it is possible that the Clp1p phosphatase may also contribute to primary septum synthesis, as Clp1p overexpression can promote septum assembly and completion of cytokinesis in cells with disrupted contractile rings (Mishra *et al.*, 2004).

MATERIALS AND METHODS

Strain construction and growth methods

Supplemental Table S1 lists the fission yeast strains used in this study. Strains were constructed by tagging genes at their endogenous loci using PCR-based gene targeting protocols (Bahler *et al.*, 1998) so fusion proteins were expressed under the control of their native promoters. Cells for microscopic studies were grown in exponential phase at 25°C in YE5S (yeast extract with amino acid supplements) liquid medium in 50-ml flasks to a density between 0.2 and 0.4 OD_{595}. Cells with genes under control of the *nmt* promoter were grown in exponential phase at 25°C for 24 h before transitioning to EMM5S (Edinburgh minimal medium with amino acid supplements) liquid medium with 15 μM thiamine to deplete protein expression for 10 h before imaging.

Microscopy

Cells were centrifuged at 500 × *g* for 1 min and washed three times with EMM5S. Cells were plated on a thin pad of 25% gelatin in EMM5S medium supplemented with 0.1 mM *n*-propyl-gallate (Wu *et al.*, 2008; Arasada and Pollard, 2011). Fluorescence images of live cells were acquired between 23 and 25°C with an Olympus IX-71 inverted microscope with a 63×/numerical aperture 1.4 Plan Apo lens, Andor Technology (Belfast, Northern Ireland) CSU-X1 confocal spinning disk confocal system, and Andor Technology iXON-EM-CCD camera. Unless otherwise noted, *Z*-stacks of 16 slices at 0.5-μm intervals were acquired at 2-min intervals with an exposure time of 100 ms. For each condition, data were collected from multiple cells in multiple experiments.

Image analysis

Image analysis was conducted with ImageJ software and macros (National Institutes of Health, Bethesda, MD). Cells expressed the fluorescently tagged protein of interest along with the spindle pole body protein Sad1p-CFP or Sad1p-RFP to place events on a time scale in which time zero is defined as separation of the spindle pole

bodies (Wu *et al.*, 2003). We defined cell cycle events as follows: transition of interphase nodes to cytokinesis nodes was the time when fluorescently tagged Cdc15p and Myo2p appeared in punctae at the middle of cells in maximum intensity projection images; formation of a complete contractile ring was when nodes condensed into a continuous ring in maximum intensity projection images and three-dimensional reconstructions; the onset of contractile ring constriction and septum deposition was when the diameter of the ring began to change; and completion of ring constriction or septum deposition was when the ring diameter stopped changing.

The numbers of GFP or YFP molecules in the cleavage furrow region were acquired by measuring the fluorescence intensity in sum images of a rectangular area enclosing the nodes or ring. The measurements were corrected for camera noise, uneven illumination, diffuse cytoplasmic fluorescence, and acquisition photobleaching (Hoffman *et al.*, 2001; Wu and Pollard, 2005). The number of molecules per pixel was calculated from a calibration curve based on the fluorescence intensity of seven mGFP or mYFP tagged proteins: capping protein (Acp2p), α-actinin (Ain1p), actin-related protein 2 (Arp2p), actin-related protein 3 (Arp3p), Arp complex protein C5 (ArpC5p), fimbrin (Fim1p), and type II myosin (Myo2p; Wu and Pollard, 2005; Wu *et al.*, 2008).

We used a log-rank test for Kaplan–Meier curves (Klein and Moeschberger, 2003; Rich *et al.*, 2010) implemented with software from MedCalc for Windows 12.7.8 (MedCalc Software, Ostend, Belgium) to compare whole outcomes curves and calculate a *p* value for a pair of curves being different. Statistical significance for molecule quantification measurements was calculated using the *t* test.

Cellular viability and growth assays

S. pombe cells were grown in YE5S liquid medium at 25°C for 24 h, diluted 1:100, and grown an additional 12 h at 25°C to maintain a population in exponential growth phase at a density between 0.2 and 0.4 OD_{595}. Equal numbers of cells were serially diluted 10-fold four times, and 5-µl aliquots were spotted onto YE5S agar plates for growth at 25, 30, or 36°C for 36–72 h. Plates were placed on a backlight box (Hall Productions, San Luis Obispo, CA), and a digital camera (Kodak DC290; Rochester, NY) was used to acquire images by transmitted light. Images were loaded into ImageJ, and colony growth was measured by densitometry using the NIH Image Gel Analyzer plug-in. Percentage growth for each condition is shown relative to wild-type growth in Table 2.

Expression and purification of Blt1p

The *S. pombe* DNA sequence encoding full-length Blt1p amino acid residues 1–700 was cloned into the *Bam*HI site of pQE80L vector (Qiagen, Valencia, CA), which added a hexahistidine tag to the C-terminus. Clones were transformed into ArcticExpress-competent cells (Stratagene, La Jolla, CA). Cells were grown at 25°C overnight to stationary phase in LB (Luria broth) medium, then diluted 1:100 into LB medium with 0.1 mg/ml ampicillin and grown at 25°C for 6 h, when 1 mM isopropyl-β-D-thiogalactoside was added to induce expression for 16 h at 10°C. In a typical preparation, cells from 8 l of culture were harvested by centrifugation and resuspended in 80 ml of bacterial lysis buffer (50 mM sodium phosphate, 300 mM NaCl, 10 mM imidazole, pH 8.0, with two protease inhibitor cocktail tablets [Roche, Basel, Switzerland]). Cells were lysed by sonication and clarified by centrifugation at 18,000 rpm for 45 min in a JA-30.50 Ti rotor (Beckman Coulter, Brea, CA). Blt1p was purified from the supernatant as follows.

Step1: Ni-NTA affinity purification. Lysates containing Blt1p-6xHis were loaded onto a 10-ml bed of Ni-NTA agarose resin (Qiagen) equilibrated with bacterial lysis buffer and washed with 50 ml of Ni-NTA wash buffer (50 mM sodium phosphate, 300 mM NaCl, 20 mM imidazole, pH 8.0). Proteins were eluted with 15 ml of Ni-NTA elution buffer (50 mM sodium phosphate, 300 mM NaCl, 250 mM imidazole, pH 8.0) and dialyzed overnight at 4°C into MonoQ buffer A (20 mM Tris, pH 8.0, 50 mM NaCl, 1 mM dithiothreitol [DTT]).

Step 2: Anion exchange chromatography. The dialyzed sample was loaded onto an 8-ml column of Mono Q 5/50GL (GE Healthcare) in MonoQ buffer A, and unbound proteins were washed out using two column volumes of MonoQ buffer A. Fractions of 0.5 ml were collected during elution with a linear salt gradient from 0 to 100% MonoQ buffer B (20 mM Tris, pH 8.0, 500 mM NaCl, 1 mM DTT) over 40 column volumes at 0.5 ml/min. The Blt1p-6xHis peak eluted at 38–48% MonoQ buffer B, corresponding to 215 mM NaCl.

Step 3: Size exclusion chromatography. Fractions 30–38 from step 2 containing Blt1p were pooled and concentrated to <1 ml with an Amicon Ultra 3000 MWCO centrifugal filter (Millipore, Billerica, MA) and purified on a 120-ml column of Superdex 200 (GE Healthcare Bio-Sciences, Piscataway, NJ) in gel filtration buffer (20 mM Tris, pH 8.0, 20 mM NaCl, 0.5 mM EDTA, 1 mM DTT). Fractions of 1.3 ml were collected over one column volume at 0.3 ml/min. Blt1p-6xHis eluted in fractions 42–48, which were pooled and concentrated to <500 µl with an Amicon Ultra 3000 MWCO centrifugal filter (Millipore). The final purified Blt1p retained the hexahistidine tag.

Analytical gel filtration

We calibrated a 24-ml column of Superdex 200 (GE Healthcare Bio-Sciences) with five purified proteins in gel filtration buffer at 0.5 ml/min: thryoglobulin, ferritin, catalase, aldolase, and serum albumin. The peak elution volume for each protein was used to calculate a partition coefficient using the formula

$$\text{Partition coefficient} = (\text{elution volume} - \text{void volume})/(\text{column volume} - \text{void volume})$$

where the total column volume was 24.4 ml and the void volume was 8.3 ml. An inverse complement error function was calculated for each protein using the Wolfram Functions Site InverseErfc program (Wolfram Research, Champaign, IL), and these values were plotted against the Stokes radius for each protein standard to obtain a formula for calculating the Stokes radius of Blt1p from its Inverse erfc partition coefficient (Akers, 1967).

Sedimentation velocity analytical ultracentrifugation

Sedimentation velocity analytical ultracentrifugation was carried out at 20°C using a Beckman XL-1 analytical ultracentrifuge. Samples of 400 µl of purified Blt1p or gel filtration buffer were loaded in two-channel centerpieces fitted with quartz windows in a four-hole rotor. Samples were centrifuged at 42,000 rpm and monitored by scanning absorbance at 280 nm along the radial length of the cell every 5 min. SEDFIT and SEDNTERP software were used to analyze the sedimentation profiles and calculate molecular weights, diffusion coefficients, density and viscosity of the buffer, and partial specific volume of the protein.

Binding experiments

S. pombe strains expressing Cdc15p-mEGFP, Mob1p-mEGFP, or Sid2p-mEGFP were grown in YE5S liquid medium at 25°C for 24 h, diluted 1:100 into 100 ml of YE5S, and grown an additional 12 h at 25°C to maintain a population in exponential growth phase at a density between 0.2 and 0.4 OD_{595}. Cultures were centrifuged at 1000 × *g* for 15 min at 25°C, and cells were washed three times in

S. pombe lysis buffer (20 mM phosphate buffer, 10 mM NaCl, 1% Triton X-100, 0.2 mM DTT, 1 mM phenylmethylsulfonyl fluoride, pH 7.4, with two Roche protease inhibitor tablets per 10-ml buffer). Cells were lysed with a bead beater (Wu and Pollard, 2005) and clarified by centrifugation at 13,000 × *g* for 15 min at 4°C. Lysates were incubated 1:1 with 150 µl of Ni-NTA agarose resin (Qiagen) in *S. pombe* lysis buffer for 30 min at 4°C on a rotary wheel. Samples were centrifuged at 1000 × g for 5 min, and supernatants were removed.

A 1:1 solution of Ni-NTA agarose resin (Qiagen) in *S. pombe* lysis buffer (200-µl total volume) was incubated with or without 10 µM Blt1p-hexahistidine for 30 min at 4°C on a rotary wheel. Ni-NTA agarose was washed three times with 200 µl of *S. pombe* lysis buffer to remove unbound Blt1p-hexahistidine. Samples of 150 µl of the precleared lysates from cells expressing Cdc15p-mEGFP, Mob1p-mEGFP, or Sid2p-mEGFP were added to the 50 µl of Ni-NTA resin and incubated at 4°C for 2 h on a rotary wheel. Samples were centrifuged at 1000 × g for 5 min, the 150-µl supernatants were removed, and 50 µl of SDS protein sample buffer (50 mM Tris-HCl, pH 6.8, 2% SDS, 10% glycerol, 1% β-mercaptoethanol, 12.5 mM EDTA, and 0.02% bromophenol blue) was added to each sample (200-µl total volume). Pelleted beads were washed three times with 150 µl of *S. pombe* lysis buffer and resuspended in 50 µl of protein sample buffer. Supernatant and pellet fractions were boiled for 5 min, loaded on a 4–20% SDS–polyacrylamide gel, and run at 120 V for 1.5 h.

Immunoblotting

Electrophoresis was used to transfer proteins from SDS–polyacrylamide gels to nitrocellulose membranes (GE Healthcare Bio-Sciences). GFP fusion proteins from *S. pombe* lysates were detected by immunoblotting (Wu and Pollard, 2005) using a 1:4000 dilution of ab290 anti-GFP primary antibody (Abcam, Cambridge, England) and 1:15,000 dilution of horseradish peroxidase–conjugated anti-rabbit secondary antibody (4050-05; Southern Biotech, Birmingham, AL). Membranes were incubated with ECL reagent (GE Healthcare Bio-Sciences), exposed to x-ray film (GE Healthcare Bio-Sciences), and developed.

ACKNOWLEDGMENTS

Research reported here was supported by National Institute of General Medical Sciences of the National Institutes of Health Award R01GM026132. The content is solely the responsibility of the authors and does not necessarily represent the official views of the National Institutes of Health. We thank Shambaditya Saha for calibrating the gel filtration column; Rajesh Arasada, Chad McCormick, and Matt Akamatsu for assistance with microscopy and image analysis; and Miriam Alonso for assistance with analytical ultracentrifugation.

REFERENCES

Akers GK (1967). A new calibration procedure for gel filtration columns. J Biol Chem 242, 3237–3238.

Almonacid M, Celton-Morizur S, Jakubowski JL, Dingli F, Loew D, Mayeux A, Chen JS, Gould KL, Clifford DM, Paoletti A (2011). Temporal control of contractile ring assembly by Plo1 regulation of myosin II recruitment by Mid1/anillin. Curr Biol 21, 473–479.

Arasada R, Pollard TD (2011). Distinct roles for F-BAR proteins Cdc15p and Bzz1p in actin polymerization at sites of endocytosis in fission yeast. Curr Biol 21, 1450–1459.

Bahler J, Wu JQ, Longtine MS, Shah NG, McKenzie A 3rd, Steever AB, Wach A, Philippsen P, Pringle JR (1998). Heterologous modules for efficient and versatile PCR-based gene targeting in *Schizosaccharomyces pombe*. Yeast 14, 943–951.

Bezanilla M, Forsburg SL, Pollard TD (1997). Identification of a second myosin-II in *Schizosaccharomyces pombe*: Myp2p is conditionally required for cytokinesis. Mol Biol Cell 8, 693–705.

Chen CT, Feoktistova A, Chen JS, Shim YS, Clifford DM, Gould KL, McCollum D (2008). The SIN kinase Sid2 regulates cytoplasmic retention of the Cdc14-like phosphatase Clp1 in S. pombe. Curr Biol 18, 1594–1599.

Clifford DM, Wolfe BA, Roberts-Galbraith RH, McDonald WH, Yates JR 3rd, Gould KL (2008). The Clp1/Cdc14 phosphatase contributes to the robustness of cytokinesis by association with anilin-related Mid1. J Cell Biol 181, 79–88.

Coffman VC, Nile AH, Lee IJ, Liu H, Wu JQ (2009). Roles of formin nodes and myosin motor activity in Mid1p-dependent contractile-ring assembly during fission yeast cytokinesis. Mol Biol Cell 20, 5195–5210.

Cortes JC, Ishiguro J, Duran A, Ribas JC (2002). Localization of the (1,3) beta-D-glucan synthase catalytic subunit homologue Bgs1p/Cps1p from fission yeast suggests that it is involved in septation, polarized growth, mating, spore wall formation, and spore germination. J Cell Sci 115, 4081–4096.

Cueille N, Salimova E, Estaban V, Blanco M, Moreno S, Bueno A, Simanis V (2001). Flp1, a fission yeast orthologue of the *S. cerevisiae* CDC14 gene, is not required for cyclin degradation or rum1p stabilisation at the end of mitosis. J Cell Sci 114, 2649–2664.

Erickson HP (2009). Size and shape of protein molecules at the nanometer level determined by sedimentation, gel filtration, and electron microscopy. Biol Proced Online 11, 32–51.

Esteban V, Blanco M, Cueille N, Simanis V, Moreno S, Bueno A (2004). A role for the Cdc14-family phosphatase Flp1p at the end of the cell cycle in controlling the rapid degradation of the mitotic inducer Cdc25p in fission yeast. J Cell Sci 117, 2461–2468.

Fankhauser C, Reymond A, Cerutti L, Utzig S, Hofmann K, Simanis V (1995). The *S. pombe* cdc15 gene is a key element in the reorganization of F-actin at mitosis. Cell 82, 435–444.

Guzman-Vendrell M, Baldissard S, Almonacid M, Mayeux A, Paoletti A, Moseley JB (2013). Blt1 and Mob1 provide overlapping membrane anchors to position the division plane in fission yeast. Mol Cell Biol 33, 418–428.

Hachet O, Simanis V (2008). Mid1p/anillin and the septation initiation network orchestrate contractile ring assembly for cytokinesis. Genes Dev 22, 3205–3216.

Hoffman DB, Pearson CG, Yen TJ, Howell BJ, Salmon ED (2001). Microtubule-dependent changes in assembly of microtubule motor proteins and mitotic spindle checkpoint proteins at Ptk1 kinetochores. Mol Biol Cell 12, 1995–2009.

Hou MC, Guertin DA, McCollum D (2004). Initiation of cytokinesis is controlled through multiple modes of regulation of the Sid2p-Mob1p kinase complex. Mol Cell Biol 24, 3262–3276.

Hou MC, Salek J, McCollum D (2000). Mob1p interacts with the Sid2p kinase and is required for cytokinesis in fission yeast. Curr Biol 10, 619–622.

Huang T, Tan H, Balasubramanian MK (2008). Assembly of normal actomyosin rings in the absence of Mid1p and cortical nodes in fission yeast. J Cell Biol 183, 979–988.

Jin QW, Zhou M, Bimbo A, Balasubramanian MK, McCollum D (2006). A role for the septation initiation network in septum assembly revealed by genetic analysis of sid2-250 suppressors. Genetics 172, 2101–2112.

Jourdain I, Brzezinska EA, Toda T (2013). Fission yeast Nod1 is a component of cortical nodes involved in cell size control and division site placement. PLoS One 8, e54142.

Klein JP, Moeschberger ML (2003). Survival Analysis: Techniques for Censored and Truncated Data, 2nd ed., New York: Springer.

Krapp A, Simanis V (2008). An overview of the fission yeast septation initiation network (SIN). Biochem Soc Trans 36, 411–415.

Laporte D, Coffman VC, Lee IJ, Wu JQ (2011). Assembly and architecture of precursor nodes during fission yeast cytokinesis. J Cell Biol 192, 1005–1021.

Le Goff X, Motegi F, Salimova E, Mabuchi I, Simanis V (2000). The S. pombe rlc1 gene encodes a putative myosin regulatory light chain that binds the type II myosins Myo3p and Myo2p. J Cell Sci 113, 4158–4163.

Le Goff X, Woollard A, Simanis V (1999). Analysis of the cps1 gene provides evidence for a septation checkpoint in *Schizosaccharomyces pombe*. Mol Gen Genet 262, 163–172.

Liu J, Wang H, Balasubramanian MK (2000). A checkpoint that monitors cytokinesis in *Schizosaccharomyces pombe*. J Cell Sci 113, 1223–1230.

Liu J, Wang H, McCollum D, Balasubramanian MK (1999). Drc1p/Cps1p, a 1,3-beta-glucan synthase subunit is essential for division septum assembly in *Schizosaccharomyces pombe*. Genetics 153, 1193–1203.
Martin SG, Berthelot-Grosjean M (2009). Polar gradients of the DYRK-family kinase Pom1 couple cell length with the cell cycle. Nature 459, 852–856.
McCormick CD, Akamatsu M, Ti SC, Pollard TD (2013). Measuring affinities of fission yeast spindle pole body proteins in live cells across the cell cycle. Biophys J 105, 1324–1335 .
Mishra M, Karagiannis J, Trautmann S, Wang H, McCollum D, Balasubramanian MK (2004). The Clp1p/Flp1p phosphatase ensures completion of cytokinesis in response to minor perturbation of the cell division machinery in *Schizosaccharomyces pombe*. J Cell Sci 117, 3897–3910.
Morrell JL, Nichols CB, Gould KL (2004). The GIN4 family kinase, Cdr2p, acts independently of septins in fission yeast. J Cell Sci 117, 5293–5302.
Moseley JB, Mayeux A, Paoletti A, Nurse P (2009). A spatial gradient coordinates cell size and mitotic entry in fission yeast. Nature 459, 857–860.
Mulvihill DP, Hyams JS (2003). Role of the two type II myosins, Myo2 and Myp2, in cytokinetic actomyosin ring formation and function in fission yeast. Cell Motil Cytoskeleton 54, 208–216.
Naqvi NI, Wong KC, Tang X, Balasubramanian MK (2000). Type II myosin regulatory light chain relieves auto-inhibition of myosin-heavy-chain function. Nat Cell Biol 2, 855–858.
Padmanabhan A, Bakka K, Sevugan M, Nagvi NI, D'souza V, Tang X, Mishra M, Balasubramanian MK (2011). IQGAP-related Rng2p organizes cortical nodes and ensures position of cell division in fission yeast. Curr Biol 21, 467–472.
Paoletti A, Chang F (2000). Analysis of mid1p, a protein required for placement of the cell division site, reveals a link between the nucleus and the cell surface in fission yeast. Mol Biol Cell 11, 2757–2773.
Pardo M, Nurse P (2003). Equatorial retention of the contractile actin ring by microtubules during cytokinesis. Science 300, 1569–1574.
Pollard TD, Wu JQ (2010). Understanding cytokinesis: lessons from fission yeast. Nat Rev Mol Cell Biol 11, 149–155.
Proctor SA, Minc N, Boudaoud A, Chang F (2012). Contributions of turgor pressure, the contractile ring, and septum assembly to forces in cytokinesis in fission yeast. Curr Biol 22, 1601–1608.
Rich JT, Neely JG, Paniello RC, Voelker CC, Nussenbaum B, Wang EW (2010). A practical guide to understanding Kaplan-Meier curves. Otolaryngol Head Neck Surg 143, 331–336.
Roberts-Galbraith RH, Ohi MD, Ballif BA, Chen JS, McLeod I, McDonald WH, Gygi SP, Yates JR3rd, Gould KL (2010). Dephosphorylation of F-BAR protein Cdc15 modulates its conformation and stimulates its scaffolding activity at the cell division site. Mol Cell 39, 86–99.
Saha S, Pollard TD (2012). Anillin-related protein Mid1p coordinates the assembly of the cytokinetic contractile ring in yeast. Mol Biol Cell 23, 3982–3992.
Salimova E, Sohrmann M, Fournier N, Simanis V (2000). The *S. pombe* orthologue of the *S. cerevisiae* mob1 gene is essential and functions in signaling the onset of septum formation. J Cell Sci 113, 1695–1704.
Sladewski TE, Previs MJ, Lord M (2009). Regulation of fission yeast myosin-II function and contractile ring dynamics by regulatory light chain and heavy chain phosphorylation. Mol Biol Cell 20, 3941–3952.
Sparks CA, Morphew M, McCollum D (1999). Sid2p, a spindle pole body kinase that regulates the onset of cytokinesis. J Cell Biol 146, 777–790.
Trautmann S, Wolfe BA, Jorgensen P, Tyers M, Gould KL, McCollum D (2001). Fission yeast Clp1p phosphatase regulates G2/M transition and coordination of cytokinesis with cell cycle progression. Curr Biol 11, 931–940.
Vavylonis D, Wu JQ, Hao S, O'Shaughnessy B, Pollard RD (2008). Assembly mechanism of the contractile ring for cytokinesis by fission yeast. Science 319, 97–100.
Wolfe BA, Gould KL (2004). Fission yeast Clp1p phosphatase affects G(2)/M transition and mitotic exit through Cdc25p inactivation. EMBO J 23, 919–929.
Wu JQ, Kuhn JR, Kovar DR, Pollard TD (2003). Spatial and temporal pathway for assembly and constriction of the contractile ring in fission yeast cytokinesis. Dev Cell 5, 723–734.
Wu JQ, McCormick CD, Pollard TD (2008). Chapter 9: counting proteins in living cells by quantitative fluorescence microscopy with internal standards. Methods Cell Biol 89, 253–273.
Wu JQ, Pollard TD (2005). Counting cytokinesis proteins globally and locally in fission yeast. Science 310, 310–314.
Wu JQ, Sirotkin V, Kovar DR, Lord M, Beltzner CC, Kuhn JR, Pollard TD (2006). Assembly of the cytokinetic contractile ring from a broad band of nodes in fission yeast. J Cell Biol 174, 391–402.
Ye Y, Lee IJ, Runge KW, Wu JQ (2012). Roles of putative Rho-GEF Gef2 in division-site positioning and contractile-ring function in fission yeast cytokinesis. Mol Biol Cell 23, 1181–1195.